

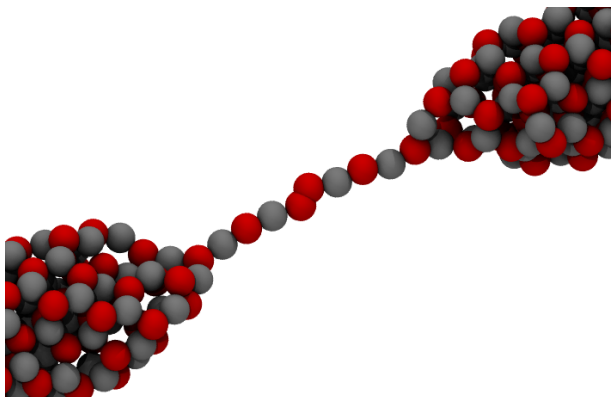
# Supporting Information

## Mechanochemical stability of sub-nm ZnO chains.

Germán J. Soldano, Franco Zanotto, Marcelo M. Mariscal\*

INFIQC - Departamento de Matemática y Física - Facultad de Ciencias Químicas Universidad Nacional de Córdoba, Argentina

\*Corresponding author: marcelo.mariscal@gmail.com



### 1. ZnO atomic chains

Formation energy is defined as

$$E_f = E_w(\text{Zn}_m\text{O}_n) - mE_{at}(\text{Zn}) - nE_{at}(\text{O}) \quad (1)$$

where  $E_w(\text{Zn}_m\text{O}_n)$  is the energy of an atomic chain of  $m$  zinc atoms and  $n$  oxygen atoms, and  $E_{at}(\text{Zn})$  and  $E_{at}(\text{O})$  the energy of zinc and oxygen isolated atoms, respectively. Four atomic chains were studied by DFT calculations in order to verify that the structures observed are indeed the most likely to form.

Fig 1 shows formation energy as a function of strain for different monoatomic ZnO chains according to DFT calculations. The most stable type of chain was found to be the one without an oxygen-oxygen bond. This is in excellent agreement with our MD simulations using the ReaxFF potential, where only one of such bonds is observed short before rupture.

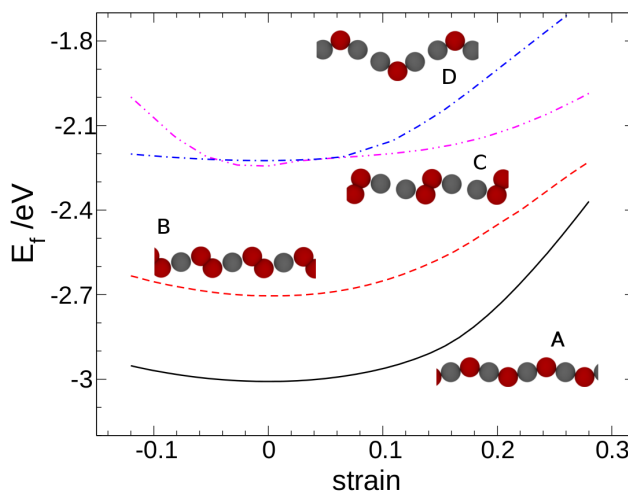


**Figure 1.** Formation energy of four types of infinite monoatomic ZnO chains as a function of strain. A side view of the chains in their relaxed configuration (strain = 0) is also shown. These chains are formed by **A**: Interspersed Zn and O atoms; **B**: O<sub>2</sub> linked by a single Zn atom; **C**: O<sub>2</sub> linked by two Zn atoms; **D**: an O atom linked by two Zn atoms.

### 2. BCK and RFF performance

In order to compare performances of RFF, BCK, and DFT on nanostructures, stretching studies on chains and ladders were carried out using these three techniques. Results are shown in Fig. 2-4 To ease the comparison, energy values has been referred to that of the equilibrium.

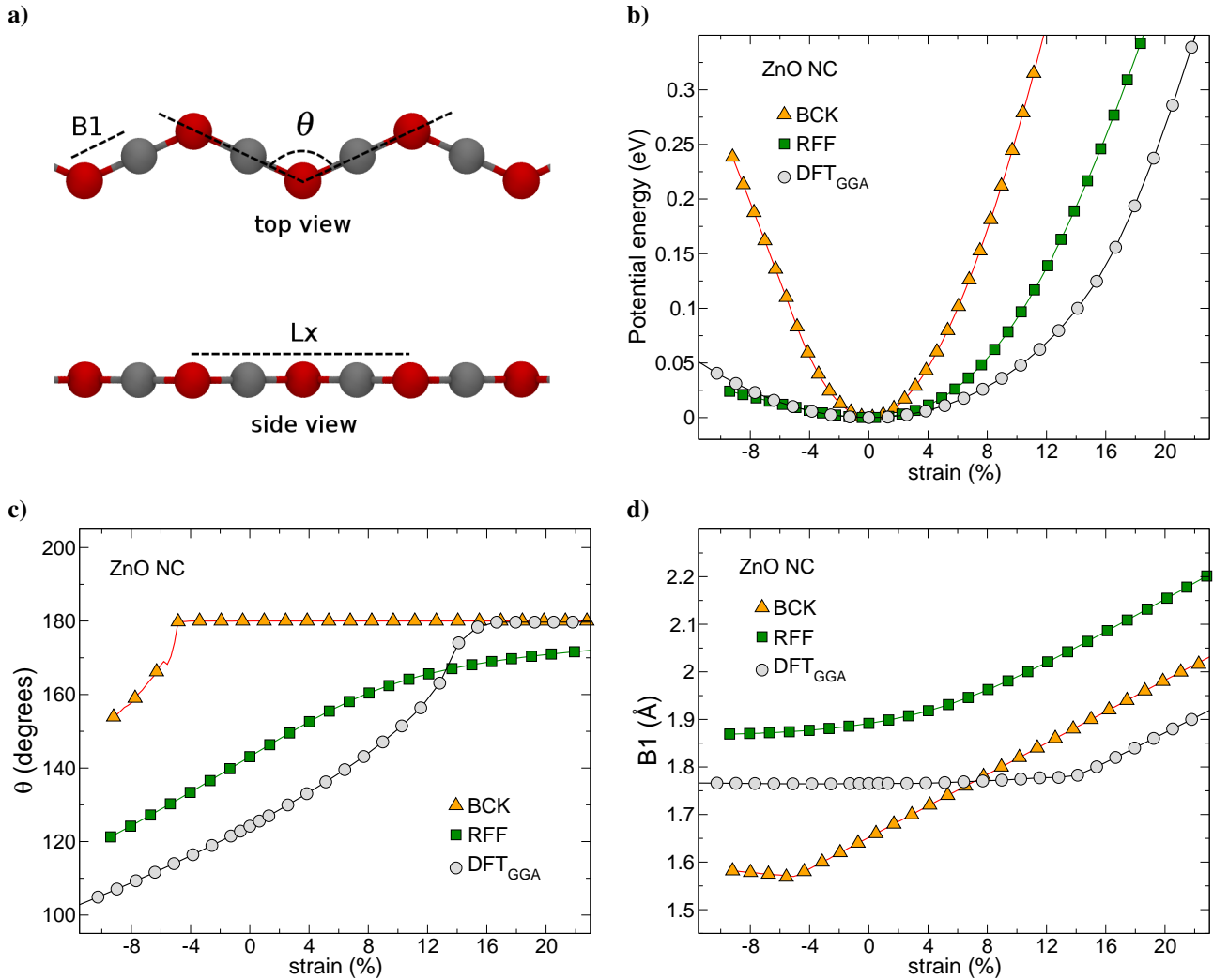


**Figure 2. Chains without O<sub>2</sub> (NC1):** Performance of Buckingham potential (BCK) and the Reactive Force Field (RFF). Energies, distances, and angles are compared with those obtained using DFT. The length of the unit cell ( $L_x$ ) is also shown. The most important outcome of these comparisons is the large energy error of BCK with respect to DFT. Another failure of the former, is the rigidity assigned to the  $\theta$  angle, which above  $-5\%$  of strain is always  $180^\circ$ .

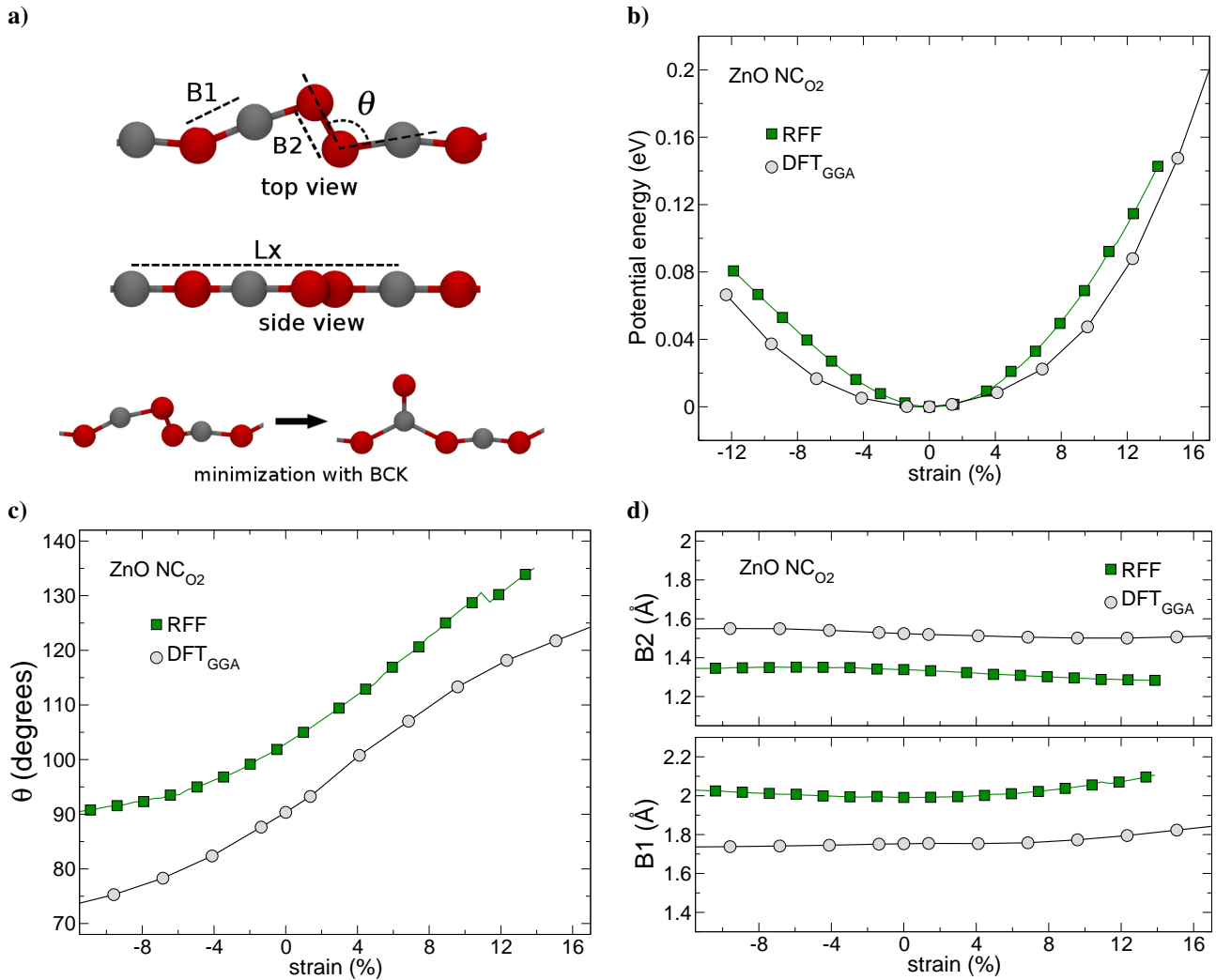


**Figure 3. Chains with O<sub>2</sub> (NC2):** Performance of Buckingham potential (BCK) and the Reactive Force Field (RFF). Energies, distances, and angles are compared with those obtained using DFT. The length of the unit cell ( $L_x$ ) is also shown. For the Buckingham potential, the oxygen-oxygen interaction implies a strong repulsion (it does not contemplate the covalent bond). As depicted in (a), energy minimizations using BCK lead to rearrangements in which the oxygen atoms are not longer bonded to each other.

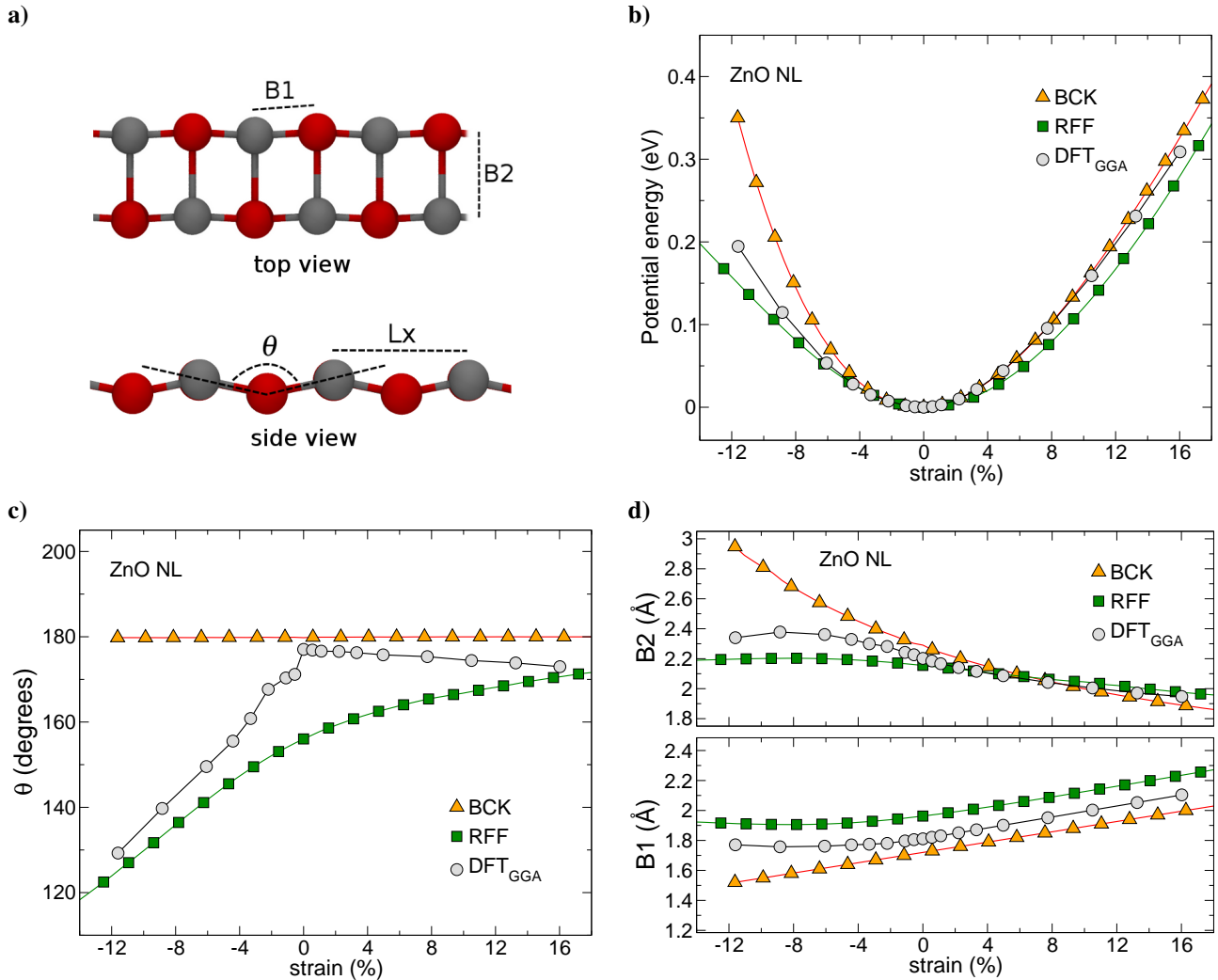


**Figure 4. Nanoladders:** Performance of Buckingham potential (BCK) and the Reactive Force Field (RFF). Energies, distances, and angles are compared with those obtained using DFT. The length of the unit cell ( $L_x$ ) is also shown. In this case the energies of both techniques are close to that of DFT, although RFF becomes more accurate at large negative strains. Again, BCK assigns an unrealistic rigidity to the  $\theta$  angle. In fact, nanoladders in the Buckingham potential are planar at any strain.

### 3. Stretching speed

In order to study the influence of the stretching speed on the chain length before rupture, statistical analysis were performed over sets of 25 MDs for  $NW_I$  and  $NW_{II}$ . Fig. 5 shows histogram of chain lengths for  $0.8\text{ m/s}$  and  $8.0\text{ m/s}$  stretching speeds.

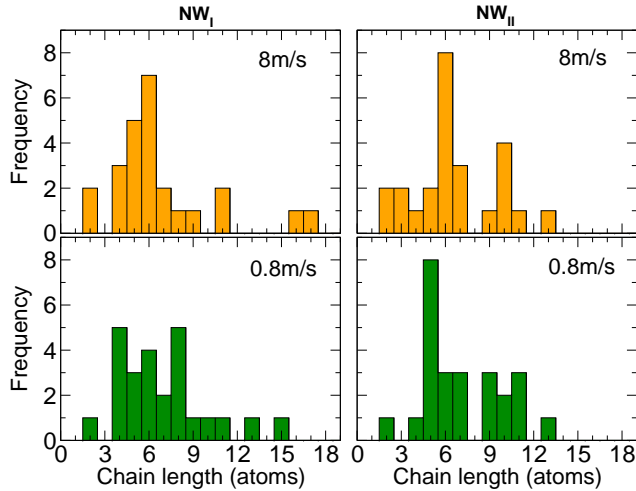


**Figure 5.** Histogram of the chain length over 25 MDs for  $0.8\text{ m/s}$  and  $8.0\text{ m/s}$  stretching velocities. Values correspond to  $NW_I$  and  $NW_{II}$  at 300 K.

The most common chain length and the maximal chain length for each nanowire at different stretching speeds show similar values. Since the strain speed seems to have little effect on the distribution of chain lengths, further calculations were performed at the fast stretching speed ( $8.0\text{ m/s}$ ).

### 4. Voronoi charges

In order to study the evolution of the charge as chains are stretched, Voronoi charges[1] were calculated for three stages of stretching: at equilibrium (A), close to chain fracture (B), and after chain rupture (C). Results are shown in Fig. 6. A negligible change on atomic charges is observed during stretching until the chain breaks. These charges are of the order of  $+1.1\text{ e}$  for zinc atoms,  $-1.1\text{ e}$  for oxygen atoms, and  $-0.55\text{ e}$  for each atom of the  $O_2$  species. This values confirm the dual nature of the oxygen bond in  $O_2$ ; each oxygen has an ionic bond with its Zn neighbor (only that with half the typical value) and a covalent bond with its oxygen partner. After rupture, terminal atoms decrease their module charge by 50%, approximately. This is simply because, when broken, they can only take or give charge from one neighbor, instead of two.

### 5. Projected density of states

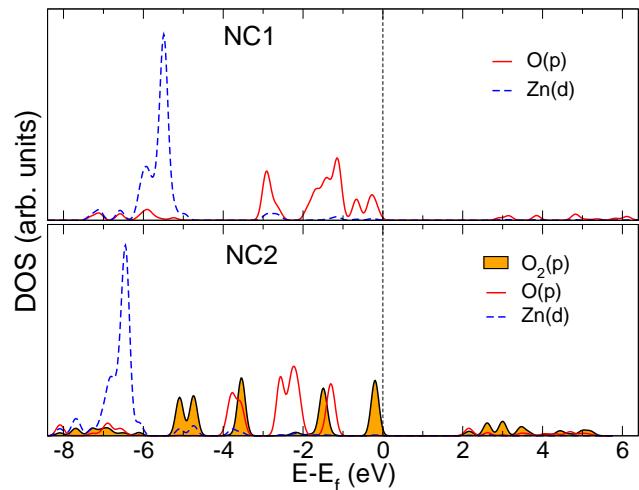


**Figure 7.** Projected density of states of ZnO nanochains. States with greater contributions to the total density of states are shown. State  $O(p)$  corresponds to oxygen atoms bonded to zinc atoms, and state  $O_2(p)$  to oxygen atoms in the  $O_2$  species. Note the the latter occupies higher energy sates than the the other oxygen atoms, increasing the Fermi level.

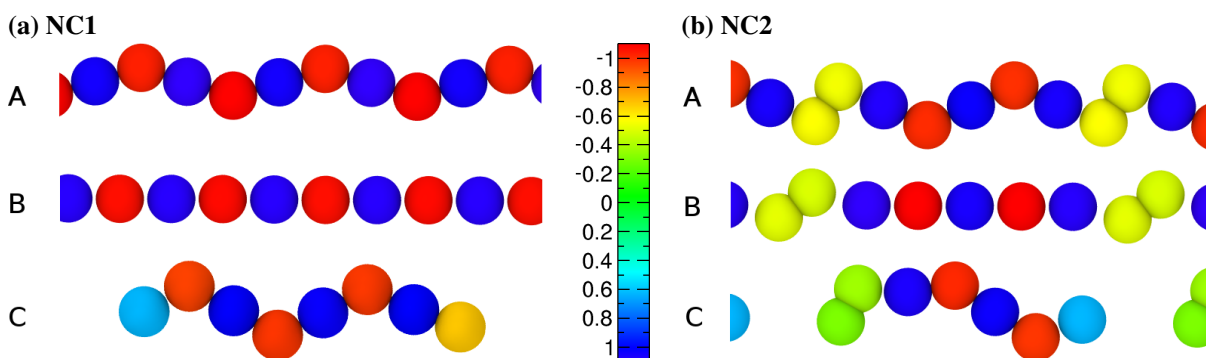


**Figure 6.** Voronoi charges of NC1 and NC2 chains at three stages of stretching. **A:** at equilibrium, **B:** close to chain fracture, **C:** after chain breaking. All negative values correspond to oxygen atoms and positive values to Zn atoms.

## References

- [1] Célia Fonseca Guerra, Jan-Willem Handgraaf, Evert Jan Baerends, and F. Matthias Bickelhaupt. Voronoi deformation density (vdd) charges: Assessment of the mulliken, bader, hirshfeld, weinhold, and vdd methods for charge analysis. *Journal of Computational Chemistry*, 25(2):189–210, 2004.